First-principles density-functional calculations on HCr$_3$O$_8$: An exercise to better understand the ACr$_3$O$_8$ (A = alkali metal) family

R. Vidya · P. Ravindran · A. Kjekshus · H. Fjellvåg

Abstract Accurate *ab initio* density-functional calculations are performed to understand structural stability, electronic structure, and magnetic properties of the ACr$_3$O$_8$ (A = H, Li, Na, K, Rb, Cs) series. The ground-state structures for the compounds with A = Li−Rb take the same KCr$_3$O$_8$-type atomic arrangement (space group $C2/m$), whereas CsCr$_3$O$_8$ adopts a modified atomic architecture (prototype; space group $Pnma$), in agreement with available experimental findings. The hypothetical compound HCr$_3$O$_8$ is found to stabilize in an LiV$_3$O$_8$-type structure (space group $P2_1/m$), with an unexpectedly large equilibrium volume. The electronic structures of the ACr$_3$O$_8$ compounds are analyzed using density-of-states, charge-density, and electron-localization-function plots, and all are found to exhibit semiconducting (insulating at 0 K) properties with very narrow band gaps. The Cr atoms occur in two different valence states and all compounds (except NaCr$_3$O$_8$) are found to exhibit antiferromagnetic ordering of magnetic moments at 0 K.

Keywords Density-functional calculations · Mixed valence · Semiconductivity · Magnetic properties

Introduction

Owing to exotic phenomena like colossal magnetoresistance (CMR) and spin, charge, and orbital ordering [1], oxides comprising transition-metal atoms in mixed-valence states attract much attention. Mixed-valence compounds with Mn,

Co, and Cu are widely studied, whereas compounds with, say, Cr and Ni are less explored. In an effort to understand better the mixed-valence Cr compounds, we have studied structural stability, electronic structure, and magnetic properties within the series ACr$_3$O$_8$ (A = H, Li, Na, K, Rb, and Cs) where Cr formally exists in two different valence states. The study has been undertaken using accurate density-functional-theory (DFT) calculations. In an earlier contribution [2] we have reported on electronic, magnetic, and bonding characteristics of ACr$_3$O$_8$ with A = Na, K, and Rb and more recently [3] we have explored the ground-state structures of Cr$_3$O$_8$ and LiCr$_3$O$_8$ which are of considerable interest in relation to cathode material for rechargeable Li-ion batteries. In the present work we consider overall trends in structural behavior, electronic structure, and magnetic properties for these compounds, with some special attention on the highly hypothetical HCr$_3$O$_8$.

Computational details

The results presented here are based on DFT calculations according to the projected-augmented plane-wave (PAW) [4] method as implemented in the VASP (Vienna *ab initio* simulation package) [5]. In this approach the valence orbitals are expanded as plane waves and the interactions between the core and valence electrons are described by pseudopotentials. In order to determine the ground-state structures for the ACr$_3$O$_8$ compounds, we have performed structural optimizations. We considered the experimentally established structures as the first choice for guess structures where such information is available. To broaden the structural platform for the series, and for compounds without explicit experimental structure data in particular, a considerable number of seemingly relevant structural arrangements were considered

R. Vidya (✉) · P. Ravindran · A. Kjekshus · H. Fjellvåg
Department of Chemistry, University of Oslo, Box 1033 Blindern, N-0315 Oslo, Norway
e-mail: vidya.ravindran@kjemi.uio.no

as test structures. The optimization of the atomic geometry is performed via a conjugate-gradient minimization of the total energy, utilizing Hellmann-Feynman forces on the atoms and stresses in the unit cell. During the simulations, atomic coordinates and axial ratios are allowed to relax for different volumes of the unit cell. These parameters are changed iteratively so that the total energy converges to a minimum value. Convergence minimum is assumed to have been attained when the energy difference between two successive iterations is less than 10^{-7} eV per cell and the forces acting on the atoms are less than 1 meV Å^{-1}. The structure with the lowest total energy is taken as the ground-state structure. The generalized-gradient approximation (GGA) [6] is used to obtain the accurate exchange and correlation energy for a particular atomic configuration. The calculations are carried out using 64 **k** points in the irreducible Brillouin zone. We have used same energy cutoff and **k**-point density in all calculations. All calculations are performed for paramagnetic (P), ferromagnetic (F), and antiferromagnetic (AF) configurations.

Results and discussion

Structural optimization

For LiCr$_3$O$_8$, a relatively old single-crystal x-ray diffraction study [7, 8] concluded with an orthorhombic (space group *Cmcm*) structure with random distribution of Li and one third of the Cr atoms over one and the same crystallographic site. In order to partially mimic such a disorder computationally, we constructed a supercell with an ordered arrangement of the Li and Cr atoms concerned. The complete random distribution of these Li and Cr atoms had to be abolished because our programs do not allow random distribution of different atoms at one site. Hence our optimizations had to end with a more regular arrangement of Li and Cr atoms than postulated by Wilhelmi [7] (the energy gain between the input and resulting relaxed structure exceeding 1.3 eV f.u.$^{-1}$). The resulting structure [designated LiCr$_3$O$_8$-II; the same space group (*C*2/*m*) as for LiCr$_3$O$_8$-I, but a somewhat different atomic arrangement] has the lowest energy compared to other structure types considered [3]. The LiCr$_3$O$_8$-I atomic arrangement, which is isostructural with that of succeeding members of the *A*Cr$_3$O$_8$ series is, in fact, found to be slightly higher in energy than LiCr$_3$O$_8$-II. The *A*Cr$_3$O$_8$ compounds with *A* = Na, K, and Rb are found to stabilize in the experimentally determined [9] KCr$_3$O$_8$-type structure [space group *C*2/*m*; *A*(Cr1)(Cr2)$_2$O$_8$] which comprises two types of Cr atoms arranged in fairly regular octahedral and tetrahedral environments of O neighbors. There are three crystallographically different O atoms. The octahedra and tetrahedra are arranged in layers parallel to the *a*, *b* plane by corner sharing. The layers are held together by alkali-metal ions.

According to our calculations, CsCr$_3$O$_8$ is found to stabilize in the prototype structure with *Pnma* symmetry in agreement with the experimental findings [10]. The atomic arrangement is similar to the KCr$_3$O$_8$-type forerunners in the *A*Cr$_3$O$_8$ series with layers of CrO$_6$ octahedra and CrO$_4$ tetrahedra joined at corners. However, the orientation of half of the tetrahedra is different, and every second layer is rotated 180° compared with the layers in the KCr$_3$O$_8$-type structure.

The *A*Cr$_3$O$_8$ structures exhibit a significant difference between the Cr—O distances in the CrO$_6$ octahedra and CrO$_4$ tetrahedra which immediately points at a mixed-valence situation for the Cr atoms, conventionally interpreted as the ionic valence states Cr^{3+} and Cr^{6+}, respectively. Rigid-band considerations and preliminary electronic structure studies on *A*Cr$_3$O$_8$ (*A* = Li—Cs) suggest insulating behavior for all members. In order to further elucidate the rigid-band deductions we also included the highly hypothetical compound HCr$_3$O$_8$ in the considerations.

Among the twelve different structural arrangements considered in the structural optimization for HCr$_3$O$_8$, the KCr$_3$O$_8$, LiCr$_3$O$_8$-II, and LiV$_3$O$_8$ (*P*2$_1$/*m*) types came out with the lower total energies. Among the tested alternatives, inputs according to the types NaNb$_3$O$_8$ (*Ibam*) and LiTa$_3$O$_8$ (*Pmma*) came out with the highest total energies; these and variants which fall in the intermediate energy range are not included in Fig. 2. The illustration shows that the LiV$_3$O$_8$-type structure has the lowest total energy ($\sim$1.62 eV f.u.$^{-1}$ lower than the KCr$_3$O$_8$-type variant), however, with a much larger equilibrium volume (191.91 vs 133.68 Å^3 f.u.$^{-1}$). Possible reasons for such an unexpected large cell volume will be discussed later. Although an HI$_3$O$_8$-type arrangement could have been a more likely structural arrangement for HCr$_3$O$_8$ from a chemical point of view, our calculations show that this variant comes out with about 6.42 eV higher total energy than the LiV$_3$O$_8$-type structure.

Optimized structural parameters for HCr$_3$O$_8$ are given in Table 1. The structure comprises three types of Cr atoms and eight types of O atoms. The three types of Cr atoms exhibit different Cr—O interatomic distances in configurations which are of the trigonal bipyramidal form. The polyhedra around Cr1 share edges whereas those around Cr2 and Cr3 share corners along the *a* direction. These polyhedra form Cr—O molecular-like units with H in intermediate positions.
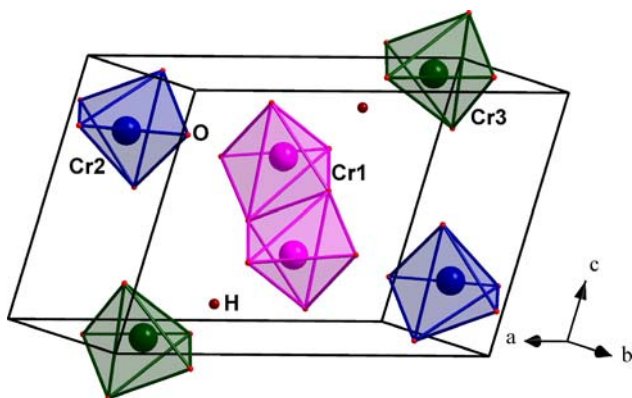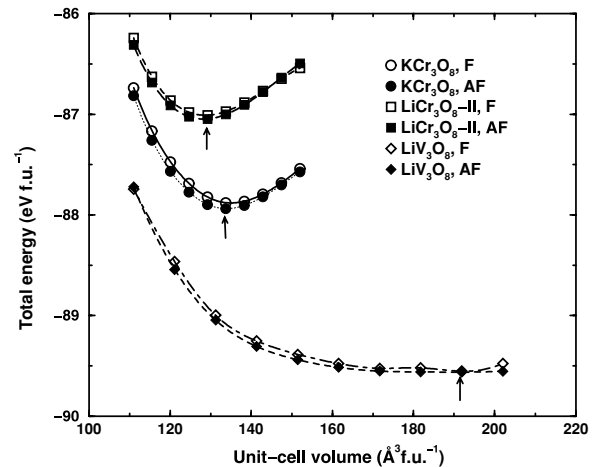
The calculated equilibrium volume for *A*Cr$_3$O$_8$ (*A* = Li—Cs) increases roughly linearly with the radius of *A*. The equilibrium unit-cell parameters vary some 2−4% from the available experimental values, viz. approaching the range of accuracy of the GGA. However, the calculated equilibrium volumes for the alkali-metal members of the *A*Cr$_3$O$_8$ series are generally too large compared with the experimental volumes (note that GGA overestimates volume by around 3 % [11]). This may originate from the somewhat open and layered nature of the structural arrangements where

Table 1 Optimized ground-state structure parameters for HCr_3O_8 in LiV_3O_8-type structure (space group $P2_1/m$; all atoms are in position $2e$ where $y = 1/4$)

Unit cell	Atom	x	z
$a = 13.8287$ Å	H	0.3022	0.8413
$b = 3.8235$ Å	Cr1	0.4741	0.6529
$c = 6.9332$ Å	Cr2	0.9148	0.7468
$\beta = 100.37°$	Cr3	0.1398	0.9714
$V = 191.91$ Å^3	O1	0.5168	0.4120
	O2	0.0951	0.2021
	O3	0.3591	0.6840
	O4	0.8486	0.5341
	O5	0.5492	0.8566
	O6	0.0458	0.7660
	O7	0.2612	0.9551
	O8	0.8665	0.9760

Fig. 2 Calculated cell volume vs total energy for HCr_3O_8. Structure-type inputs are specified on the illustration. Arrow points at total-energy minimum

interlayer interactions are more governed by van der Waals forces which are unfortunately not accounted for properly in the DFT calculations of today.

The equilibrium volumes for HCr_3O_8 in the $LiCr_3O_8$-II- and KCr_3O_8-type structural arrangements fit reasonably well into the approximately linear relation between ionic radius of A and cell volume for the ACr_3O_8 compounds with alkali-metal cations (Fig. 3). However, the total energy for these variants is much higher than that for the ground-state LiV_3O_8-type structure (see Fig. 2). On the other hand, the cell volume for the ground-state (LiV_3O_8-type) atomic arrangement is so high that it is not really comparable with the findings for the other compounds at all. A likely inference of these findings is that a compound like HCr_3O_8 would be so acidic that it should not be possible to stabilize it in a salt-like structure. Another fact which must be taken into account is that the structure prescribed for our hypothetical HCr_3O_8 (Fig. 1) consists of molecular-like Cr-to-O

Fig. 1 The optimized crystal structure of HCr_3O_8 in LiV_3O_8-type atomic arrangment. Crystallographically different Cr atoms are labeled on the illustration

iono-covalent-bonded subunits. Hence, when the hydrogen and their chromium-oxygen counterparts atoms are allowed to relax, they may arrange themselves relatively freely in an "abundance" of space. It should also be mentioned that experimental studies [12] on Li intercalation in Cr_3O_8 have shown that when the concentration of Li is increased, the intercalated "$LiCr_3O_8$" framework gradually becomes amorphous. The unexpected large equilibrium volume observed for HCr_3O_8 with LiV_3O_8-type structure may be an omen indicating that "such a compound" really prefers the amorphous state.

Magnetic properties

The structural optimizations performed for P, F, and AF configurations show that all compounds stabilize in the AF state, except $NaCr_3O_8$. The calculated AF ground state for KCr_3O_8 is in agreement with the magnetic susceptibility data [13, 14] which shows AF ordering below a Néel temperature of 125 $\pm$ 4 K. Magnetic property data are not available for the other compounds.

The magnetic moment values listed for HCr_3O_8 in Table 2 refer both to the LiV_3O_8-type ground-state structure and the excited-state KCr_3O_8-type arrangement, the latter to facilitate comparison with the ACr_3O_8 compounds of the alkali metals. Owing to Cr-d and O-p hybridization, the oxygen atoms also possess small magnetic moments, resulting in somewhat higher total moments than the sum of the Cr moments in the F case. The different magnetic moments immediately support different valence states for the Cr atoms in these compounds, and at first sight the findings appear to confirm the formal electron-counting picture that Cr1 corresponds to Cr^{3+} (d^3) and Cr2 to Cr^{6+} (d^0). However, a closer investigation of the bonding situation reveals that the assignment of formal valence states to Cr in these compounds is non-trivial.

Fig. 3 Equilibrium volume for the ACr$_3$O$_8$ series as a function of ionic radius of A (standard values). The data for HCr$_3$O$_8$ expose volumes for LiV$_3$O$_8$-, KCr$_3$O$_8$-, and LiCr$_3$O$_8$-II-type structural arrangements (see Fig. 2)
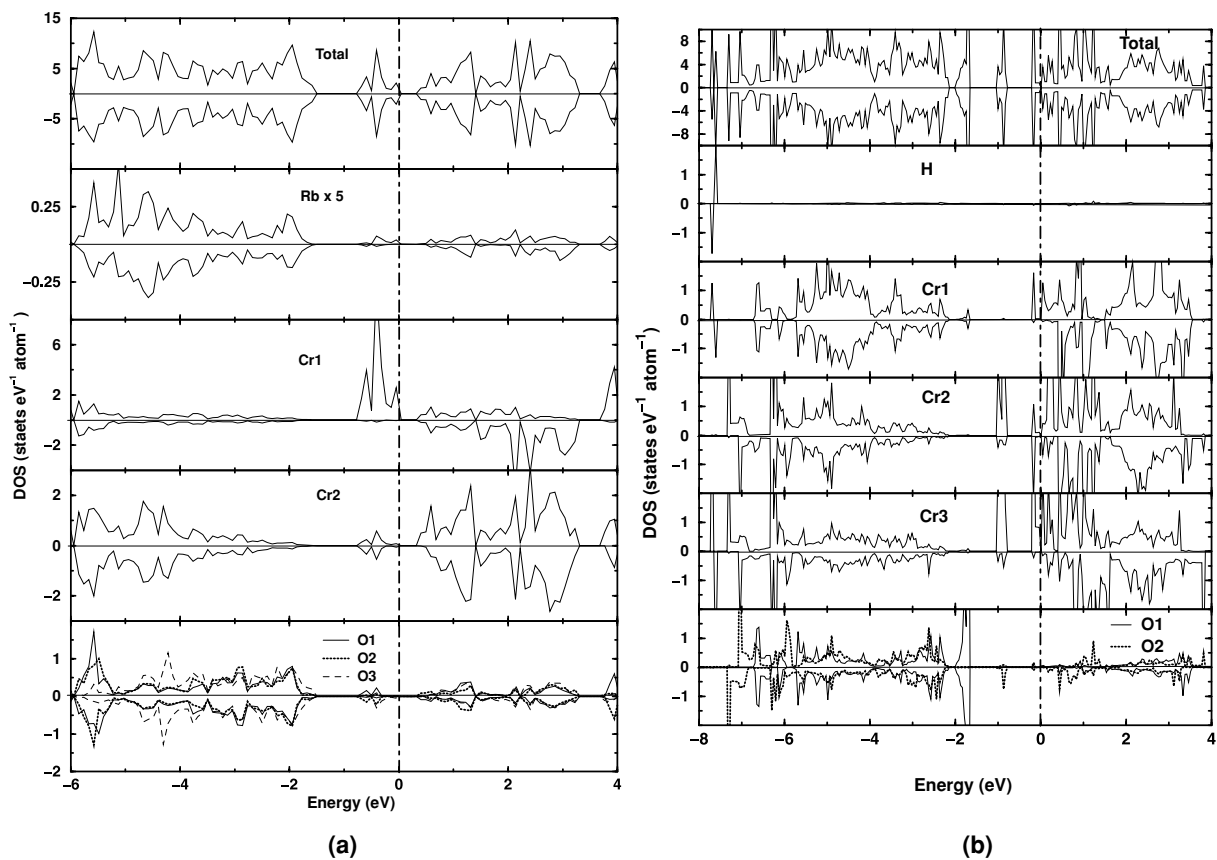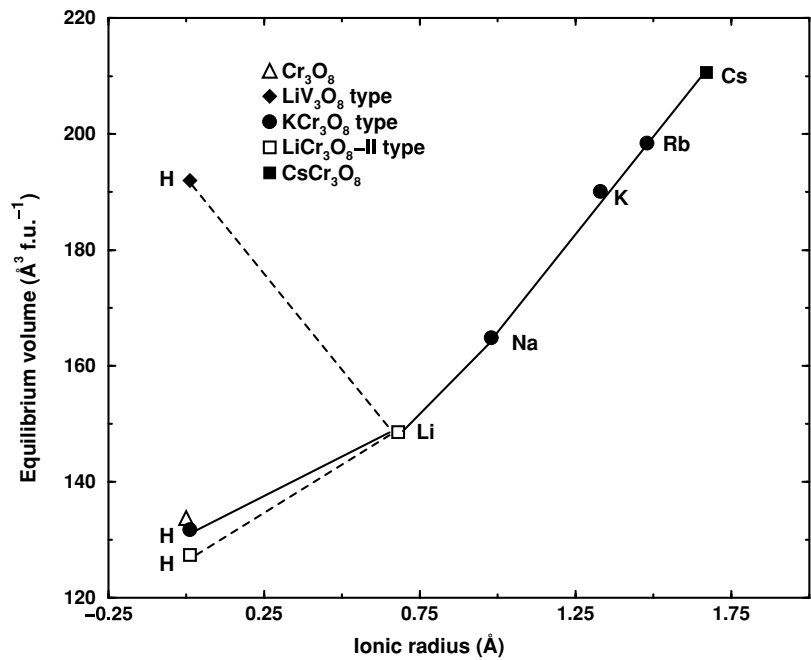

Fig. 4 Total and site-projected density of states for (a) RbCr$_3$O$_8$ in KCr$_3$O$_8$-type (note the increased scale for Rb) and (b) HCr$_3$O$_8$ in LiV$_3$O$_8$-type structures; both in AF state. The Fermi level is indicated by vertical dashed lines

Table 2 Calculated magnetic moment (in μ_B per Cr atom) for ACr$_3$O$_8$ compounds in F and AF states. Total refers to the total magnetic moment per formula unit

Compound	F			AF	
	Cr1	Cr2	Total	Cr1	Cr2
HCr$_3$O$_8$[a]	0.390	1.394	2.878	0.348	1.448
HCr$_3$O$_8$[b]	2.566	0.207	2.857	2.507	0.004
LiCr$_3$O$_8$	2.600	0.222	2.886	2.578	0.032
NaCr$_3$O$_8$	2.451	0.241	2.868	2.391	0.013
KCr$_3$O$_8$	2.449	0.228	2.859	2.330	0.016
RbCr$_3$O$_8$	2.453	0.224	2.857	2.336	0.003
CsCr$_3$O$_8$	2.478	0.238	2.867	2.479	0.237

[a]LiV$_3$O$_8$-type structure; Cr3 moment 1.521 and 1.282 μ_B in F and AF states, respectively.
[b]KCr$_3$O$_8$-type structure.

Electronic structure

The compounds under consideration are all semiconductors (insulators at 0 K) with very small band gaps (E_g ranging from 0.12 to 0.63 eV). The hypothetical HCr$_3$O$_8$ would exhibit the smallest $E_g = 0.12$ eV, in agreement with rigid-band considerations. As the band structure of these compounds exhibit similar features we only display the total and site-projected DOS profiles for the ground-state structures of RbCr$_3$O$_8$ and HCr$_3$O$_8$ (Fig. 4). Figure 4(a) shows that RbCr$_3$O$_8$ is a semiconductor with $E_g = 0.33$ eV. In common with A for the other ACr$_3$O$_8$ compounds, the Rb states are almost empty (visible only after appreciable multiplication) emphasizing pronounced ionic character. Cr and O states are energetically degenerate indicating considerable covalent interaction between them.

The different valence states of Cr are also evident from the differences in their DOS curves. The majority-spin chan-nel for Cr1 (Cr2 and Cr3 for HCr$_3$O$_8$) has more occupied states than the corresponding minority-spin channel demonstrating larger exchange splitting and hence a sizeable magnetic moment(s). Moreover, if Cr2 (Cr1 for HCr$_3$O$_8$) really had been in the Cr^{6+} (d^0) state it should have exhibited an empty d band. Instead, it shows a considerable number of well-localized states with more or less equal occupancy in both spin channels. Hence for Cr2 (Cr1 for HCr$_3$O$_8$) it can be inferred that its almost zero magnetic moment is not due to a genuine Cr^{6+} (d^0) state, but results from negligible exchange splitting. All crystallographically different O atoms have states in the same energy region, but they display significant topological differences in the DOS curves.

Bonding in HCr$_3$O$_8$

In order to gain understanding of the unusually large equilibrium volume for the ground-state structure of HCr$_3$O$_8$, we display charge-density (distribution of charges in real space) and electron-localization-function (ELF; see Refs. [15, 16]) plots in Fig. 5. A distinct charge density at the H site indicates that it retains some localized electronic charge which does not participate in bonding interaction with the other constituents of HCr$_3$O$_8$. On the other hand, large charges seen between Cr1 and the surrounding O atoms as well as a substantial ELF at O directed toward Cr1 imply strong covalent interaction. The large value and spherical shape of the ELF at H, lead one to believe that H remains more or less aloof as H$^{\delta+}$ ($\delta < 1$) in the structure whereas the chromium and oxygen atoms form distinct, iono-covalent-bonded subunits in a somewhat open structure. The result appears to provide a reasonable explanation of the unexpected much larger volume for LiV$_3$O$_8$-type ground-state structure than for the KCr$_3$O$_8$- and Li$_3$O$_8$-II-type variants of HCr$_3$O$_8$.
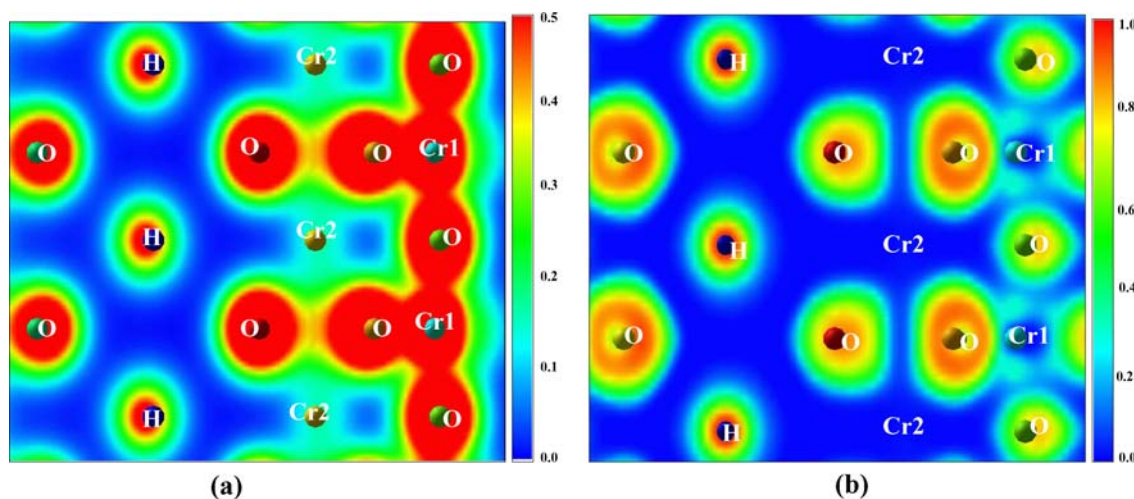

Fig. 5 Calculated (a) charge-density and (b) electron-localization-function plots for the ground-state structure of HCr$_3$O$_8$

Conclusions

From accurate first-principles density-functional calculations, it is found that the hypothetical HCr_3O_8 compound stabilizes in an LiV_3O_8-type atomic arrangement, ACr_3O_8 with $A = Li-Rb$ in KCr_3O_8-type frameworks, and $CsCr_3O_8$ in an orthorhombic (prototype) structure. The theoretically calculated ground-state structures for $NaCr_3O_8$, KCr_3O_8, $RbCr_3O_8$, and $CsCr_3O_8$ are in good agreement with available experimental results. The Cr atoms in all these compounds occur in two different valence states, one kind having large and the other small or negligible exchange splittings. All these compounds are found to be semiconductors with very small band gaps. The somewhat aloof nature of H in the ground-state structure of HCr_3O_8 and the formation of Cr-to-O iono-covalent-bonded subunits arise as possible explanations for its large equilibrium volume.

From our calculation exercise on the hypothetical HCr_3O_8 compound we have learnt the following: Although "H^+" is believed to be considerably smaller than the alkali-metal ions, the volume of the ground-state structure of HCr_3O_8 suggests that "H^+" under equilibrium condition takes up an effective size comparable with that of K^+. However, in the excited-state KCr_3O_8- and $LiCr_3O_8$-II-type structures the volume of "H^+" appears to be comparable with that of the "formal vacancy" in Cr_3O_8 with a K-stripped-off KCr_3O_8-type structure. This stresses the significance of the structural arrangement in this kind of considerations. The LiV_3O_8-type ground-state structure of HCr_3O_8 comprises distinct Cr-to-O iono-covalent-bonded subunits with "H^+" at somewhat aloof locations in the lattice whereas the KCr_3O_8-type structure exhibits characteristic chromium-oxygen layers with alkali-metal ions in between. This distinction also manifests itself in the charge distribution. The hydrogen atoms in HCr_3O_8 retains some of the charge of its valence electron whereas the valence electrons of the alkali-metal constituents in ACr_3O_8 are scarcely visible at the A sites in DOS and charge-density plots, emphasizing a more significant ionic contribution from the alkali-metal representatives to the compound formation.

The findings for HCr_3O_8 show that the magnetic features of the ACr_3O_8 series originate largely from the Cr_3O_8 subunits and that the A constituents have negligible impact on the magnetic properties. It is interesting to note that it is just $A = $ H and Cs (viz. " the small and large cations") which do not manage to keep the KCr_3O_8-type structure.

References

1. C.N.R. Rao and A.K. Raychauduri, In *Colossal Magnetoresistance, Charge Ordering, and Related Properties of Manganese Oxides*, edited by C.N.R. Rao and B. Raveau (World Scientific, Singapore, 1998).
2. R. Vidya, P. Ravindran, P. Vajeeston, H. Fjellvåg, and A. Kjekshus, *Phys. Rev.* B, **72**, 014411 (2005).
3. R. Vidya, P. Ravindran, A. Kjekshus, and H. Fjellvåg, *Phys. Rev. B* (accepted).
4. P.E. Blöchl, *Phys. Rev. B* **50**, 17953 (1994); G. Kresse and D. Joubert, *Phys. Rev. B* **59**, 1758 (1999).
5. G. Kresse and J. Furthmuller, *Comput. Mater. Sci.,* **6**, 15 (1996).
6. J.P. Perdew, K. Burke, and Y. Wang, *Phys. Rev. B*, **54**, 16533 (1996); J.P. Perdew, K. Burke, and M. Ernzerhof, *Phys. Rev. Lett.,* **77**, 3865 (1996).
7. K.-A. Wilhelmi, *Arkiv Kemi*, **6**, 131 (1967); *Chem. Commun*, 437 (1966).
8. K.-A. Wilhelmi, Doctoral Thesis, University of Stockholm (Stockholm, 1966); *Acta Chem. Scand.*, **22**, 2565 (1968).
9. M.J. Saavedra, C. Parada, and E.J. Baran, *J. Phys. Chem. Solids*, **57**, 1929 (1996).
10. K.-A. Wilhelmi, *Acta Chem. Scand.*, **12**, 1065 (1958).
11. U. Häussermann, H. Blomqvist, and D. Noréus, *Inorg. Chem.*, **41**, 3684 (2002).
12. Y. Takeda, R. Kanno, T. Tsuji, and O. Yamamoto, *J. Electrochem. Soc.*, **131**, 2006 (1984).
13. W. Klemm, *Z. Anorg. Allg. Chem.,* **301**, 323 (1959).
14. H. Fjellvåg, Unpublished results.
15. P. Ravindran, P. Vajeeston, R. Vidya, A. Kjekshus, and H. Fjellvåg, *Phys. Rev. Lett.*, **89**, 106403 (2002).
16. A. Savin, R. Nesper, S. Wengert, and T. Fässler, *Angew. Chem. Int. Ed. Engl.*, **36**, 1809 (1997).